Constructing adequate predictions for photon-atom scattering: A composite approach

J. P. J. Carney and R. H. Pratt
Department of Physics and Astronomy, University of Pittsburgh, Pittsburgh, Pennsylvania 15260

(Received 18 November 1999; published 9 June 2000)

Recent high-precision experimental results for photon scattering from neon ($\approx 1\%$ accuracy) have indicated that even present sophisticated *S*-matrix results are not sufficient to obtain agreement, even though the photon energies involved were many times the innermost threshold energy. In this case the discrepancy was traced to the use of local exchange and the neglect of electron-correlation effects. Here we present a general scheme for applying corrections to the *S*-matrix results to account for nonlocal-exchange effects and electron-correlation effects, so as to obtain results expected to be accurate at the 1% level in all elements for such energies. The corrections are based on results in simpler approximations: the form-factor approximation for elastic Rayleigh scattering, and the impulse and incoherent-scattering-factor approximations for inelastic Compton scattering. The case of scattering from neon is investigated in detail for all scattering angles and for photon energies in the range 1–100 keV. The scheme breaks down below ≈ 1 keV for elastic scattering and at low momentum transfers for inelastic scattering. We also discuss the validity of the simpler approximations, particularly the use of the impulse approximation in describing Compton scattering.

PACS number(s): 32.80.Cy

I. INTRODUCTION

The possibility of performing high-precision experiments using synchrotron sources has led to new experimental results which surpass the precision of currently available predicted results for photon-atom scattering [1]. This suggests the need for a careful consideration of the accuracy of the present methods and tabulations, and the need to develop a method for improving on these results. In Ref. [1] it was shown that for scattering from neon, for photon energies in the range 11–22 keV, a composite result derived by combining information from various present available results was sufficient at the 1% level (whereas any single result was not). Here we consider this method more generally, for all scattering angles and for photon energies in the range 1–100 keV for Rayleigh and Compton scattering from neon. We also discuss the inclusion of inelastic Raman scattering contributions, when appropriate, as well as what can be expected in elastic and inelastic scattering from other elements.

The most sophisticated calculations available for describing the dynamics of scattering are *S*-matrix calculations, available both for the elastic Rayleigh [2,3] and the inelastic Compton [4,5] scattering process (and also useable for Raman scattering [6]). The approximations made in these calculations are mainly approximations in the atomic model, which is described in terms of transitions in an independent-particle approximation (IPA), using a self-consistent Dirac-Slater-type central potential. They therefore neglect nonlocal-exchange effects and electron-correlation effects. This is well known to cause serious problems in the region of the atomic thresholds and strong anomalous scattering. However, our concern is the significance of these neglected effects in the above-threshold region, where their importance is less well appreciated. Short of a (full many-body-type) calculation that includes these effects in an intrinsic fashion, we show that it is possible in the above-threshold region to correct the *S*-matrix results for the omitted nonlocal-exchange effects and electron-correlation effects with (perturbative) corrections obtained from results in simpler (than *S*-matrix) approximations.

Here we briefly outline our methodology; for more details see Sec. II. We take the simplest models of Rayleigh and Compton scattering to be the form-factor (FF) approximation and the impulse approximation (IA), respectively. By comparing results using different wave functions one can see the effects of nonlocal exchange, electron correlations, and using relativistic versus nonrelativistic wave functions. We speak of dynamic effects as those obtained by going beyond the simplest model to a full evaluation of the photon-electron interaction Hamiltonian. The ''simplest'' predictions for scattering are defined as those obtained using the simplest models with nonrelativistic wave functions using local exchange. We regard the four effects (dynamic, nonlocal-exchange, electron-correlation, and relativistic effects) as independent perturbative corrections to the ''simplest'' predictions.

How one obtains the best prediction for the Rayleigh or Compton scattering cross section from the corresponding ''simplest'' result can be symbolically represented as

$$\left(\frac{d\sigma}{d\Omega}\right)_{\text{best}}=\left(\frac{d\sigma}{d\Omega}\right)_{\text{simplest}}\left(1+\sum_i \delta_i\right), \tag{1}$$

where the summation is over all four corrections δ_i (dynamic, nonlocal-exchange, electron-correlation, and relativistic effects). The present local relativistic *S*-matrix results should be connected to the ''simplest'' results through

$$\left(\frac{d\sigma}{d\Omega}\right)_{S\text{ matrix}}=\left(\frac{d\sigma}{d\Omega}\right)_{\text{simplest}}(1+\delta_{\text{dynamic}}+\delta_{\text{relativistic}}). \tag{2}$$

Note that this equation can be inverted to deduce the simplest results from the local relativistic *S*-matrix results.

We can of course take our starting point as the local relativistic *S*-matrix calculations, in which case the best predictions are obtained as

$$\left(\frac{d\sigma}{d\Omega}\right)_{\text{best}} = \left(\frac{d\sigma}{d\Omega}\right)_{S\text{ matrix}} (1+\delta_{\text{nonlocal}}+\delta_{\text{correlation}}). \quad (3)$$

We describe Eqs. (1)–(3) as a ''composite'' approach to the description of scattering cross sections. As we will see, the assumption that the corrections δ_i are all small fails for neon for elastic scattering below ≈ 1 keV, and for inelastic scattering at low momentum transfers, so that in such situations the composite approach will not be valid.

In the next section we discuss our methodology in more detail, and we outline the present methods and tabulations that are available. In Secs. III and IV we consider the elastic Rayleigh and inelastic Compton scattering processes, respectively, with the correction factors δ_i being given for scattering from atomic neon for all scattering angles and for photon energies in the range 1–100 keV. In Sec. V we compare the best predictions we now achieve for the cross sections with other presently available cross sections. The behavior of the corrections with Z, and further effects, such as the inclusion of unresolved Raman scattering contributions, are considered in Sec. VI, and conclusions are presented in Sec. VII.

II. CURRENTLY AVAILABLE METHODS AND THE COMPOSITE APPROACH

As mentioned in the preceding section, we take the simplest models of Rayleigh and Compton scattering to be the form-factor (FF) approximation and the impulse approximation (IA), respectively. These models are based on the A^2 term of the nonrelativistic photon-electron interaction Hamiltonian

$$H = -\frac{e}{mc}\,\boldsymbol{p}\cdot\boldsymbol{A} + \frac{e^2}{2mc^2}A^2, \quad (4)$$

and both of them have the advantage that they depend only on the bound-state electron wave function and a single variable rather than energy and angle separately. [One also has the inelastic-scattering-factor (ISF) approximation for Compton scattering, also based on the A^2 term.] The ''simplest'' predictions for scattering are taken as being those obtained using the simplest models with nonrelativistic wave functions and using local exchange. (Note that these ''simplest'' predictions may not be readily available.) By taking different choices for the wave functions, one sees the effects on the cross sections of nonlocal exchange, electron correlations, and using relativistic versus nonrelativistic wave functions.

Dynamic effects are those obtained by going beyond the simplest model to a full evaluation of the interaction Hamiltonian (4). Nonrelativistically, the FF corresponds to the exact evaluation of the A^2 term in Eq. (4). Therefore, nonrelativistically the Rayleigh dynamic term is simply the contribution of the $\boldsymbol{p}\cdot\boldsymbol{A}$ term in Eq. (4). While the IA is based on the A^2 term, further approximations are made, so that it is not an exact A^2 calculation (and neither is the ISF). The Compton dynamic term is therefore comprised of both the contribution of the $\boldsymbol{p}\cdot\boldsymbol{A}$ term and the difference between the IA and the exact evaluation of the A^2 term.

By analyzing the contributions of these four effects on scattering (dynamic, nonlocal-exchange, electron-correlation, and relativistic effects), regarding them as independent perturbative corrections to the ''simplest'' predictions for the cross section in the above-threshold region, we may correct any given result for the effects it does not include. It should be noted that the currently available results for scattering, described below, include various among (but not all of) these four effects. In particular, our analysis shows how to correct the S-matrix results for the nonlocal-exchange and electron-correlation effects they neglect, and where this procedure is valid. Note that even when starting from the S-matrix results it will still be necessary to verify the smallness of the dynamic and relativistic corrections, even though they are incorporated in the S-matrix calculation, in order to justify the assumption that nonlocal-exchange and electron-correlation corrections can be estimated from the various A^2-based results. (We must show that the dynamic effect is small so that nonlocal-exchange and electron-correlation effects in the dynamic terms may be neglected. Since many of the A^2-based results use nonrelativistic wave functions, and the separation of the A^2 term itself occurs in the nonrelativistic approximation, we must also show that relativistic effects are small, for the same reasons.) The analysis also serves to indicate the validity of other, perhaps simpler approximations, and to show circumstances in which they might perform better than the present (uncorrected) S-matrix results, due in some cases to (partial) cancellations among the corrections.

We will only consider scattering cross sections that are singly differential in the scattered photon angle. For elastic Rayleigh scattering the final photon energy is fixed, but for inelastic Compton scattering there is a spectrum of final photon energies which must be integrated over to get the singly differential cross section. We will integrate over a range that includes all of the Compton peak, but not the infrared divergent region which is present for very low scattered photon energies. We note that the ISF approximation (which we use in estimating the Compton correction effects) omits the infrared terms and implicitly performs an integration over all scattered photon energies (since closure properties are used); it could not be used if we wished to discuss correction effects in more-differential cross sections.

We now briefly review the current methods and tabulations available to use for photon-atom scattering. More details, including discussions of experimental studies, can be found in Ref. [2] for Rayleigh scattering and Ref. [7] for Compton scattering.

The present S-matrix results for Rayleigh scattering [2,3] build on the earlier work of Johnson and Feiock [8] and Brown *et al.* [9], and they have been compared extensively with experiments in the above-threshold regime. The Rayleigh S-matrix calculation can be performed for photon energies as high as ≈ 5 MeV, though for outer subshells, where the photon energy is much greater than the subshell threshold energy, the simpler (modified) form-factor approximation is usually employed [2]. The corresponding Compton S-matrix calculation [4,5] is more recent, following earlier attempts by Whittingham [10,11] and Wittwer [12]. It

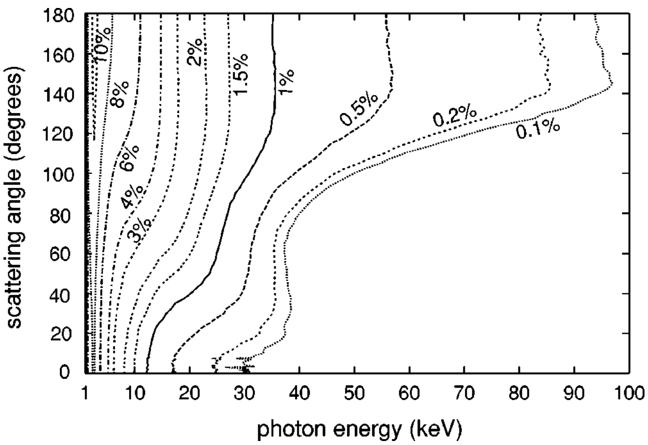

FIG. 1. Dynamic correction for Rayleigh scattering from neon.

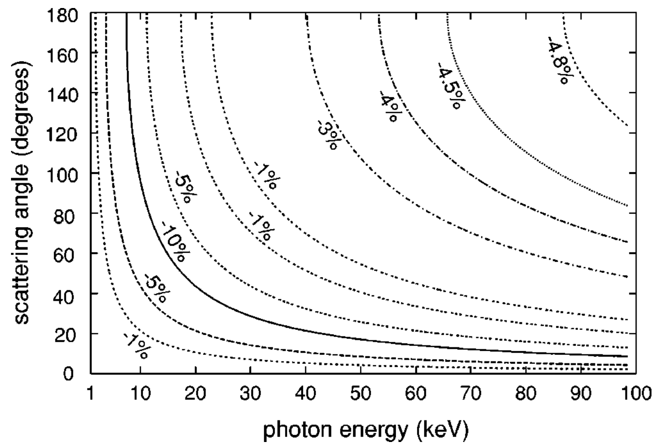

FIG. 2. Nonlocal-exchange correction for Rayleigh scattering from neon.

will fail in the Compton peak region for energies large compared to subshell binding energies. For the case of scattering from neon, the Compton S-matrix calculation is generally available in the peak region for the energies considered only for the innermost (K) shell, requiring the use of other approximations to describe the L-shell Compton peak, such as the IA and the ISF approximation, or an exact A^2 calculation (as discussed in Ref. [7]).

Many tabulations of FF's are available, using nonrelativistic bound-state wave functions in a local central potential [13], or nonlocal Hartree-Fock wave functions [14], or also including electron-correlation effects on wave functions [15]. There are corresponding results using relativistic local Dirac-Fock-Slater [16] and nonlocal Dirac-Fock wave functions [17]. Of importance for higher-Z atoms is the modified form factor (MFF) [16,18,19], which takes account of additional binding effects, needed to get the correct high-energy limit at forward angle. For Compton scattering there are IA results for the Compton profile, using both nonrelativistic [20] and relativistic [21] Hartree-Fock wave functions, and there are ISF results using nonrelativistic Hartree-Fock wave functions [14], or nonrelativistic correlated wave functions [15].

III. ELASTIC RAYLEIGH SCATTERING

We consider in turn the four corrections to Rayleigh scattering in neon: dynamic effects, nonlocal-exchange effects, electron-correlation effects beyond Hartree-Fock, and relativistic effects on the wave functions. Each is given as a percentage correction to be applied to a cross section not including that effect (assuming them all to be linearly independent perturbations). We then discuss strategies for obtaining the ''best available'' prediction for the Rayleigh-scattering cross section.

In Fig. 1 the dynamic correction is shown for neon, for all scattering angles, and for photon energies in the range 1–100 keV. This is the correction to be applied to a FF-based cross section to take account of dynamic effects. It was obtained by a comparison of S-matrix results and results obtained using the FF approximation, with relativistic wave functions in the same atomic potential. The correction is getting large at 1 keV, as the region of the atomic thresholds is being approached, where anomalous scattering is dominant. We therefore would not expect a perturbative composite scheme to yield very accurate results below 1 keV for neon, as it does not account for nonlocal-exchange and electron-correlation effects in anomalous scattering, which can be important there. For fixed energy the Rayleigh dynamic correction increases as a percentage effect on the cross sections with increasing scattering angle in all cases. This is because the anomalous contribution decreases more slowly with increasing angle than the FF contribution, leading to the anomalous terms accounting for more of the scattering cross section at larger scattering angles. (In fact, one often does well taking the anomalous scattering factors to be completely angle-independent [16].) We see that the dynamic effects are generally decreasing with increasing energy (as the anomalous scattering factors are decreasing with energy), though anomalous scattering can be important at high energy for large scattering angles for high Z.

The FF-derived nonlocal-exchange correction for neon is shown in Fig. 2, again for all scattering angles and for photon energies in the range 1–100 keV. This correction is obtained by a comparison of the nonlocal relativistic FF's of Hubbell and Øverbø [17] and FF's calculated in a local relativistic potential [16]. Since this correction is derived from FF's, it depends only on momentum transfer rather than on energy and scattering angle separately. Therefore, the contour lines in Fig. 2 are also contours of constant momentum transfer. The neon nonlocal-exchange correction is most important for the momentum transfer $x=0.56$ Å^{-1}, being a -10% correction. It is of course small at low energies and small scattering angles (low momentum transfer), since in the FF approximation the forward amplitude is simply equal to $-Z$ for any charge density.

Note that for large momentum transfers the FF is determined by the small distance behavior of the s-state wave functions (primarily the K-shell wave function). Therefore, the high-momentum-transfer limit can be understood in terms of the ratios of the normalizations for s states evaluated using nonlocal and local exchange (i.e., using the Hartree-Fock and Hartree-Fock-Slater approximations). These ratios have been investigated by Scofield [22]. In the high-

TABLE I. $F_{\mathrm{HF,HFS}}$ are the sums over s states of the square of the bound-state normalization for each s state times the number of electrons in each s state, using nonlocal Hartree-Fock and local Hartree-Fock-Slater wave functions, respectively, as described in the text. The high-momentum-transfer limit of the nonlocal Rayleigh correction $\delta_{\mathrm{nonlocal}}|_{x\to\infty}=(F_{\mathrm{HF}}^2-F_{\mathrm{HFS}}^2)/F_{\mathrm{HFS}}^2$, as described in the text.

Z	$F_{\mathrm{HF}}=\Sigma_{s\ \mathrm{states}}n_e N_{\mathrm{HF}}^2$	$F_{\mathrm{HFS}}=\Sigma_{s\ \mathrm{states}}n_e N_{\mathrm{HFS}}^2$	$\delta_{\mathrm{nonlocal}}\|_{x\to\infty}$
2	1.412	1.472	−7.9%
3	1.741	1.911	−17.0%
4	2.129	2.324	−16.2%
5	2.302	2.509	−15.8%
6	2.420	2.605	−13.7%
7	2.504	2.664	−11.7%
8	2.568	2.704	−9.8%
9	2.619	2.732	−8.1%
10	2.659	2.753	−6.7%
11	2.774	2.872	−6.7%
12	2.935	3.057	−7.9%
18	1.763	1.820	−6.3%
36	2.257	2.305	−4.1%
54	2.706	2.760	−3.9%

momentum-transfer limit the FF for an s state will be proportional to the square of the normalization N for the state, and the total FF will be proportional to the sum over all s states of the square of each s-state normalization N times the number of electrons in that s state n_e, i.e., proportional to $F=\Sigma_{s\ \mathrm{states}}n_e N^2$. (Nonrelativistically, states other than s states do not contribute in the high-momentum-transfer limit. There are in fact relativistic corrections that only become important for high Z.) Using the results of Scofield [22], we give in Table I for various Z the quantities F_{HF} and F_{HFS} based on the Hartree-Fock and Hartree-Fock-Slater approximations, respectively. Since the FF is squared to give the cross section, the high-momentum-transfer limit of the nonlocal-exchange correction is given by $\delta_{\mathrm{nonlocal}}|_{x\to\infty}=(F_{\mathrm{HF}}^2-F_{\mathrm{HFS}}^2)/F_{\mathrm{HFS}}^2$. This gives the high-momentum-transfer limit of the nonlocal-exchange correction for neon as -6.7%, which is being approached slowly. Generally this limit is decreasing in magnitude as one goes to higher Z, but it remains significant. The increase in magnitude as one goes from $Z=2$ (-7.9%) to $Z=3$ (-17.0%) is due to the $2s_{1/2}$ contribution. These is a corresponding discernible, but less evident, behavior as one goes above $Z=10$, due to the $3s_{1/2}$ contribution.

The FF-derived electron-correlation correction for neon is shown in Fig. 3, again for all scattering angles and for photon energies in the range 1–100 keV. This correction is obtained by a comparison of nonlocal nonrelativistic FF's [14] and configuration-interaction nonrelativistic FF's [15]. Therefore, these electron correlations are defined relative to the Hartree-Fock approximation, which includes the nonlocal-exchange effect. As such, this electron-correlation correction can only be meaningfully applied to a cross section once the nonlocal-exchange correction is also included (unless it is already intrinsically included). The electron-

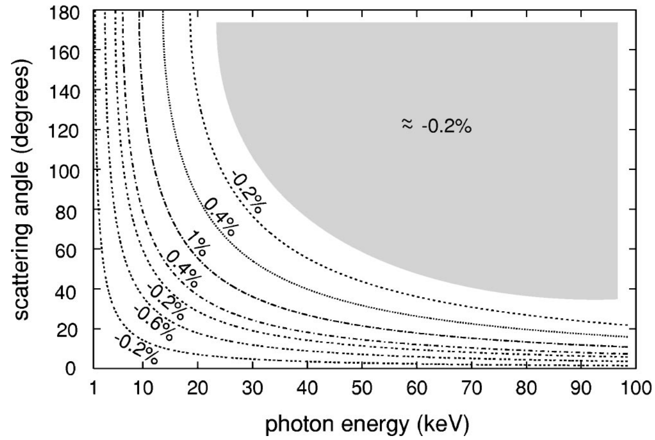

FIG. 3. Electron-correlation correction for Rayleigh scattering from neon.

correlation correction in neon is most important for the momentum transfer $x=0.77$ Å^{-1}, but it is still only $\approx 1\%$. It is of course small at low energies and small scattering angles (low momentum transfer), as for the nonlocal-exchange correction, and it reaches a value of $\approx -0.2\%$ for large momentum transfers (denoted by the shaded region).

The relativistic correction for neon is shown in Fig. 4. This correction is obtained by comparing cross sections based on FF's evaluated using relativistic [17] and nonrelativistic [14] wave functions. Generally this effect is small, becoming significant only at large momentum transfer.

We reiterate that one should not apply the dynamic correction of Fig. 1 and the relativistic correction of Fig. 4 to the Rayleigh S-matrix results, as both dynamic and relativistic effects are already included in that calculation. Rather, these corrections indicate the suitability of the FF-derived nonlocal-exchange and electron-correlation corrections of Figs. 2 and 3, respectively. By the time the dynamic correction exceeds 10% (below ≈ 1 keV in neon), the perturbative FF-based estimate of nonlocal-exchange and electron-correlation effects is in doubt.

The conclusion for elastic scattering from neon is that for

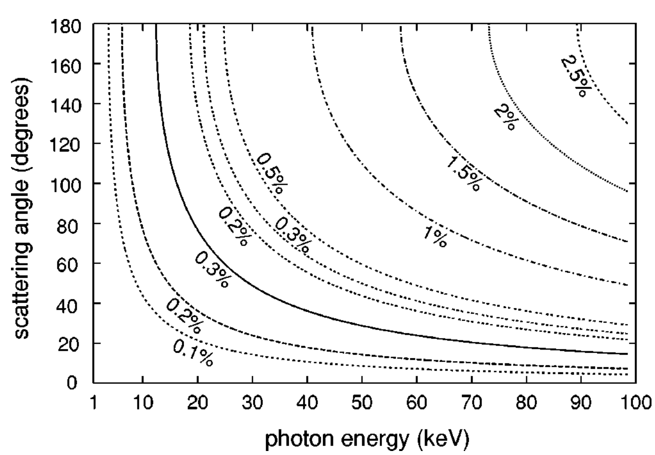

FIG. 4. Relativistic correction for Rayleigh scattering from neon.

energies greater than ≈ 1 keV, the use of FF-derived nonlocal-exchange and electron-correlation corrections to S-matrix predictions is appropriate. These corrections have a maximum magnitude of $\approx 10\%$ and they persist in the high-energy, large-scattering-angle regime (with an asymptotic value $\approx -7\%$). A comparison of Figs. 1–4 also explains why simple FF's using local exchange can perform well, as we see from the fact that there is a tendency for cancellation among the positive dynamic (and relativistic), negative nonlocal exchange, and positive-and-negative electron-correlation effects. At low energy dynamic effects are dominant; at higher energies there are circumstances in which nonlocal-exchange effects are dominant.

IV. INELASTIC COMPTON SCATTERING

As we have just done for Rayleigh scattering, we now consider in turn the four corrections to Compton scattering in neon: dynamic effects, nonlocal-exchange effects, electron-correlation effects beyond Hartree-Fock, and relativistic effects on the wave functions. Each is given as a percentage correction to be applied to a cross section not including that effect (assuming them all to be linearly independent perturbations). As discussed in Sec. II, the inelastic cross section we are considering is integrated over the spectrum of final photon energies so as to include the entire contribution of the Compton peak, but with a low-energy cutoff so as to exclude the infrared divergent region seen in Compton scattering for very low scattered photon energies (see Refs. [4,23] for a discussion of this effect). Note that these low-energy contributions are due nonrelativistically to the $\boldsymbol{p}\cdot\boldsymbol{A}$ term—in the A^2 approximation (or approximations based on the A^2 term) the scattering cross-section differential in the final photon energy becomes negligible away from the peak region. Therefore, the only correction that will be sensitive to the low-energy cutoff employed (assuming it is sufficiently low to include the whole of the Compton peak region) will be the contribution of the $\boldsymbol{p}\cdot\boldsymbol{A}$ term to the dynamic Compton correction. We note that relativistic effects are generally negligible for Compton scattering for this low-Z element, so we do not include a graph of them.

The Compton dynamic correction is composed of two terms which behave very differently: (i) the difference between an exact A^2 calculation and the result obtained using IA, and (ii) the contribution of the $\boldsymbol{p}\cdot\boldsymbol{A}$ term. We will separately consider the contributions from an A^2 calculation beyond IA and the $\boldsymbol{p}\cdot\boldsymbol{A}$ contributions to the net dynamic Compton correction. We find that the dominant contribution is given by the difference between IA and an exact A^2 calculation. The $\boldsymbol{p}\cdot\boldsymbol{A}$ term is most important for the K shell, which still only contributes at the $<1\%$ level, and it vanishes at large momentum transfers and also at sufficiently low energies, where the K shell does not contribute to inelastic Compton scattering due to its large binding energy. In Fig. 5 the dynamic A^2 correction to IA is shown for neon, for all scattering angles, and for photon energies in the range 1–100 keV. At large momentum transfers this correction is small, and the IA is expected to be valid. The correction steadily increases with decreasing momentum transfer, eventually becoming large enough that our assumption of linearly independent perturbations will not be valid. This, however, is a regime in which Compton cross sections are becoming small. In Fig. 6 the dynamic $\boldsymbol{p}\cdot\boldsymbol{A}$ correction is shown for neon, for all scattering angles, and for photon energies in the range 1–100 keV. For the energies considered here, the K-shell contribution dominates (since we are far enough above the L-shell thresholds that their $\boldsymbol{p}\cdot\boldsymbol{A}$ contributions are small). At large energies the $\boldsymbol{p}\cdot\boldsymbol{A}$ dynamic correction is negligible (except at very forward angles, but the net inelastic cross section is small there). At sufficiently low energies ($\lesssim 2$ keV), the effect is also small as inelastic scattering from the K shell is kinematically forbidden. In the intermediate regime the $\boldsymbol{p}\cdot\boldsymbol{A}$ contribution can matter at the few-tenths-of-a-percent level.

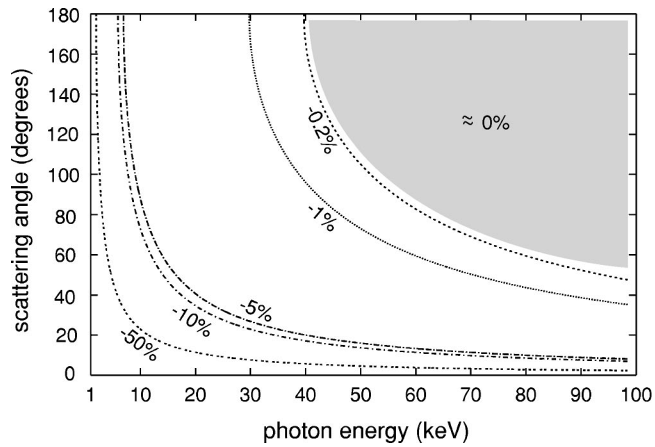

FIG. 5. Dynamic A^2 correction to impulse approximation for Compton scattering from neon.

The IA-derived nonlocal-exchange correction for neon is shown in Fig. 7, again for all scattering angles and for photon energies in the range 1–100 keV. Within IA one defines the Compton profile for the atom, which is related to the differential (in scattered photon energy and angle) inelastic scattering cross section. This is then integrated over the spectrum of final photon energies, including the whole of the Compton peak, in order to get the inelastic scattering cross

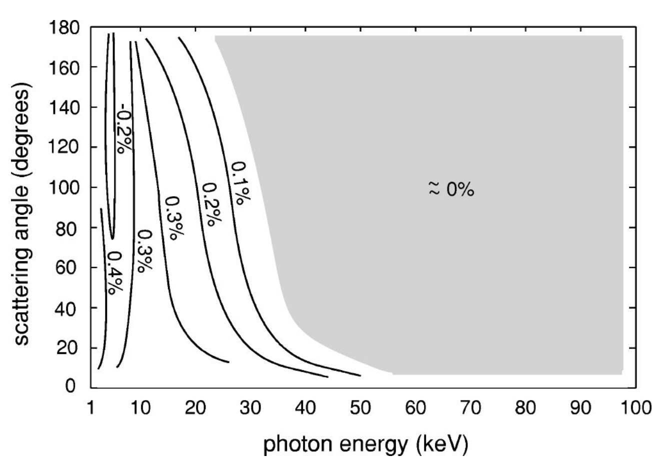

FIG. 6. Dynamic $\boldsymbol{p}\cdot\boldsymbol{A}$ correction for Compton scattering from neon.

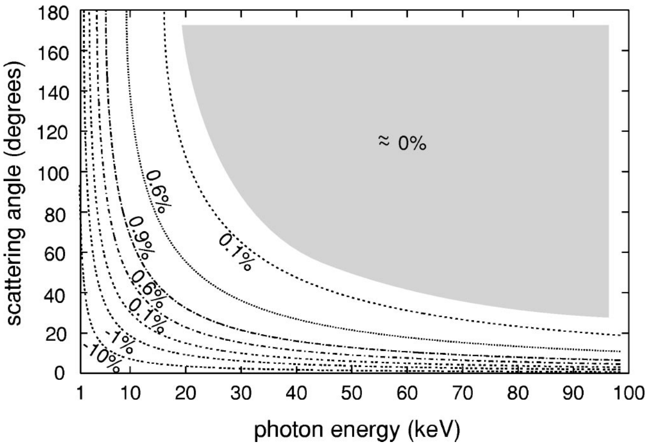

FIG. 7. Nonlocal-exchange correction for Compton scattering from neon.

section singly differential in the scattered photon angle that we consider here. The nonlocal-exchange correction is obtained here by a comparison of the Compton profile evaluated using relativistic Dirac-Hartree-Fock wave functions [24] with the corresponding Compton profile evaluated using local exchange. Converse to the situation for elastic scattering, for inelastic scattering the nonlocal-exchange correction is generally unimportant, giving contributions of $\pm 1\%$ or less, though it is larger at low momentum transfers (where the Compton cross section is becoming small). The nonlocal-exchange correction vanishes at high momentum transfers, being a tenth-of-a-percent or less effect for momentum transfers $x \approx 1.3$ Å^{-1} or larger.

The ISF-derived electron-correlation correction for neon is shown in Fig. 8, again for all scattering angles and for photon energies in the range 1–100 keV. Again, converse to elastic scattering, the electron-correlation correction can be important in inelastic scattering. This correction is obtained by a comparison of nonrelativistic Hartree-Fock ISF's [14] and configuration-interaction nonrelativistic ISF's [15]. Therefore, electron correlations are being defined relative to the Hartree-Fock approximation, which already includes nonlocal exchange. As such, the electron-correlation correction can only be meaningfully applied to a cross section once the nonlocal-exchange correction has been included (unless it is already intrinsically included). The electron-correlation correction in neon is most important for the momentum transfer $x = 0.24$ Å^{-1}, being $\approx -11\%$. However, as one goes to low momentum transfers, the Compton cross section itself is becoming small, so these effects will not be so important in total scattering cross sections, which will be dominated by elastic scattering. The electron-correlation correction to the inelastic cross section becomes unimportant at large momentum transfers, being a one-tenth-of-a-percent or less effect for momentum transfers $x \approx 3.0$ Å^{-1} or larger.

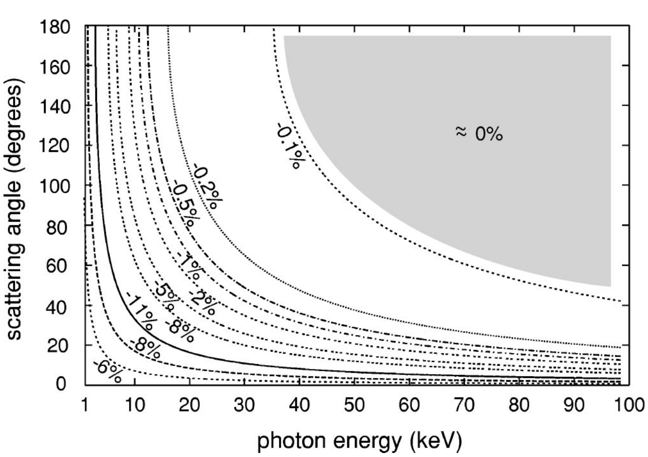

FIG. 8. Electron-correlation correction for Compton scattering from neon.

As mentioned already, the relativistic correction to the inelastic scattering cross section is generally small, being a one-tenth-of-a-percent or less effect in cross sections for momentum transfers $x \approx 0.1$ Å^{-1} or larger. At smaller momentum transfers it can be larger, but this is the regime in which the inelastic cross section is becoming small, and the assumption of linearly independent perturbations is no longer valid.

The conclusion for inelastic scattering from neon is that the use of nonlocal-exchange and electron-correlation corrections (derived within the IA and the ISF approximation) to *S*-matrix predictions is appropriate for momentum transfers large enough that the dynamic Compton correction can be considered a perturbative effect. The nonlocal-exchange and electron-correlation corrections together have a maximum magnitude of $\approx 11\%$ and vanish in the high-energy, large-scattering-angle regime (as inelastic scattering becomes more and more like scattering from a free electron). At low momentum transfers (including the forward direction at all energies) the IA and the ISF approximation fail, as does this composite approach, since the assumption of independent perturbations is no longer valid. However, in this regime the cross section for inelastic scattering itself is becoming small in comparison with the cross section for elastic scattering.

V. CROSS SECTIONS

In Table II we compare our ''best'' predictions for the elastic Rayleigh and inelastic Compton cross sections with local IPA *S*-matrix results and results based on the tabulation of Hubbell *et al.* [14], which gives nonrelativistic Hartree-Fock FF's and ISF's. Cross sections are given for five energies (1.486 keV, 5.415 keV, 11.22 keV, 27.47 keV, and 59.54 keV) and four angles (0°, 45°, 90°, and 180°), which are sufficient to indicate the general trends. We note that in all results for elastic scattering we include the contribution of the coherent nuclear Thomson amplitude for elastic scattering off the nucleus, which can matter at the 1% level for large momentum transfers (see also Ref. [25] regarding our usage of the tabulation in Ref. [14]).

The first thing to note from Table II are the regimes of dominance of the elastic and inelastic processes, seen by comparing the orders of magnitude of the Rayleigh results (columns 3–5) with those of the Compton results (columns 6–8) for the various energies and angles considered. Clearly, Rayleigh scattering is dominant at the lower energies at all angles, as well as at forward angle for higher energies, where

TABLE II. Comparison of the composite (best) predictions for the cross sections of elastic and inelastic scattering from neon with local IPA *S*-matrix predictions and with predictions based on nonlocal nonrelativistic FF's and ISF's, as described in the text. The deviations from the ''best'' predictions are shown in parentheses. For inelastic scattering at 0° the composite scheme breaks down, and the local IPA *S*-matrix prediction is intended to give only the order of magnitude.

Energy (keV)	Angle (degrees)	Elastic Rayleigh (mbarns/sr) Best	*S* matrix	Hubbell	Inelastic Compton (mbarns/sr) Best	*S* matrix	Hubbell
1.486	0	8528	8528 (0%)	7945 (−6.8%)		0.1	0
1.486	45	6225	6231 (0.1%)	5789 (−7.0%)	7.34	8.77 (19.5%)	10.98 (49.6%)
1.486	90	3879	3906 (0.7%)	3605 (−7.1%)	17.06	19.06 (11.7%)	23.63 (38.5%)
1.486	180	7099	7185 (1.2%)	6568 (−7.5%)	64.97	71.87 (10.6%)	87.95 (35.4%)
5.415	0	8241	8241 (0%)	7945 (−3.6%)		2.6	0
5.415	45	4332	4434 (2.4%)	4169 (−3.8%)	92.60	103.0 (11.2%)	115.1 (24.3%)
5.415	90	1475	1574 (6.7%)	1399 (−5.2%)	143.4	158.3 (10.4%)	170.9 (19.2%)
5.415	180	1500	1645 (9.7%)	1384 (−7.7%)	402.0	429.9 (6.9%)	461.1 (14.7%)
11.22	0	8039	8039 (0%)	7945 (−1.2%)		0.9	0
11.22	45	1737	1872 (7.8%)	1709 (−1.6%)	250.1	273.9 (9.5%)	290.9 (16.3%)
11.22	90	270.4	301.8 (11.6%)	261.7 (−3.2%)	271.0	277.7 (2.5%)	286.1 (5.6%)
11.22	180	255.3	272.8 (6.9%)	242.7 (−4.9%)	590.9	593.3 (0.4%)	606.9 (2.7%)
27.47	0	7957	7957 (0%)	7945 (−0.2%)		0.4	0
27.47	45	205.4	221.8 (8.0%)	205.6 (0.1%)	465.6	464.2 (−0.3%)	473.5 (1.7%)
27.47	90	55.84	56.40 (1.0%)	55.25 (−1.1%)	323.6	324.2 (0.2%)	329.1 (1.7%)
27.47	180	53.77	54.70 (1.7%)	52.82 (−1.8%)	617.1	619.0 (0.3%)	627.1 (1.6%)
59.54	0	7940	7940 (0%)	7945 (0.1%)		0.3	0
59.54	45	61.77	62.46 (1.1%)	61.98 (0.3%)	522.3	523.3 (0.2%)	524.3 (0.4%)
59.54	90	5.661	5.860 (3.5%)	5.639 (−0.4%)	318.7	319.3 (0.2%)	320.0 (0.4%)
59.54	180	1.964	2.057 (4.8%)	1.930 (−1.7%)	529.9	530.4 (0.1%)	533.2 (0.6%)

Compton scattering is suppressed. At the higher energies Compton scattering dominates at finite angle. We note that at forward angle ($\theta=0°$) our composite approach for inelastic Compton scattering breaks down completely, since the Compton cross section vanishes at forward angle in the IA and the ISF approximation, so that Compton scattering becomes an entirely dynamic effect (as we have defined it). Therefore, we only give the local IPA *S*-matrix predictions for Compton scattering at forward angle, which are seen to be small both in comparison to the corresponding Rayleigh cross section and to the Compton cross section at finite angle.

Concentrating on the elastic Rayleigh cross sections (columns 3–5), we consider the deviations (given in parentheses in the table) of the local IPA *S*-matrix results (column 4) and the results of Hubbell *et al.* [14] (column 5) from our ''best'' predictions (column 3). The differences between the local IPA *S*-matrix results and the ''best'' results are due to nonlocal-exchange and electron-correlation effects, the most important of which is nonlocal exchange. Therefore, the deviations in this case can be almost completely ascribed to the momentum-transfer-dependent nonlocal-exchange correction of Fig. 2, which gives rise to a maximum deviation of $\approx 10\%$, and a deviation at the highest energy of $\approx 5\%$. The differences between Hubbell *et al.* [14] and the ''best'' results can be understood at the lower energies as being entirely due to the neglect of dynamic effects (since relativistic effects are unimportant at the lower energies), causing Hubbell *et al.* [14] to underestimate the cross section. Looking at forward angle, this effect is seen to drop off with increasing energy, as the dynamic terms become less important compared to the constant forward-angle FF contribution. At a given energy, however, the neglected dynamic terms become more important with increasing angle, as the FF drops off faster than the anomalous terms. Therefore, the deviation of Hubbell *et al.* [14] increases with increasing angle for fixed energy, as seen in Table II. At higher energies in this low-*Z* element the dynamic correction is becoming unimportant.

Turning now to the inelastic Compton cross sections (columns 6–8), we again consider the deviations (given in parentheses in the table) of the local IPA *S*-matrix results (column 7) and the results of Hubbell *et al.* [14] (column 8) from our ''best'' predictions (column 6). The differences between the local IPA *S*-matrix results and the ''best'' results are due to nonlocal-exchange and electron-correlation effects, with the nonlocal-exchange correction being important only at the lowest energies or angles. Otherwise the deviations in this case can be almost completely ascribed to the momentum-transfer-dependent electron-correlation correction of Fig. 8, which gives rise to a maximum deviation of $\approx 11\%$. We should note that at the lower energies the dynamic Compton corrections are sufficiently large that our assumptions of linearly independent corrections are breaking down. Both the nonlocal-exchange and the electron-correlation corrections are becoming small for large momentum transfers, and the local IPA *S*-matrix and ''best'' results are seen to be in good agreement at the higher energies for finite angle. The deviation of Hubbell *et al.* [14] from the ''best'' result is essentially due to the dynamic Compton correction. This correction is getting large for low momentum transfers, as seen for the lower energies and for 11.22 keV for $\theta=45°$, and it is entirely responsible for the (small) finite cross sections at forward angle. At larger momentum transfers Hubbell *et al.* [14] gets better and better, as seen for the higher energies at finite angle. We finally note that the ISF result of Hubbell *et al.* [14] is a complicated result from our perspective; it includes excitation channels (i.e., Raman scattering, which we discuss in the next section) as well as ionization (since the closure properties used in its derivation involve transitions to all final states), and the final photon energy is approximated by the initial photon energy, thus allowing closure to be invoked. See Refs. [7,14,20] for discussions of the approximations made in the IA and the ISF approximation.

VI. FURTHER ISSUES

We now discuss three further issues: (i) additional aspects of the observed cross sections, such as the inclusion of Raman scattering, (ii) the expected behavior with *Z* of the corrections for different atoms, and (iii) strategies for dealing with the regimes where our approach breaks down.

In making predictions to compare with an observation made to a precision of 1% or better, one must ensure that one compares with what is actually being observed, which will in general depend on the resolution in energy. An example is the measurement of ratios of elastic to inelastic scattering in neon, and ratios of total scattering in neon to that in helium, as given in Ref. [1]. Observed cross sections may include Raman scattering as well as Rayleigh or Compton scattering. Raman scattering predictions based on the A^2 term of the photon interaction Hamiltonian (4) using nonrelativistic Coulombic wave functions have been given by Schnaidt [26], and one can also perform local IPA *S*-matrix calculations [6], as for Rayleigh and Compton scattering. In the experiment [1] the energy resolution was such that Raman scattering from the *L* shell was included with the elastic scattering, while Raman scattering from the *K* shell was included with the inelastic scattering. Consequently, it was necessary to include estimates of the Raman cross sections, though they were found to be small (and so for Raman scattering it is not necessary to consider the perturbative effects). Note that since the inelastic ISF result of Hubbell *et al.* [14] includes both ionization and excitation, one would have to subtract out the *L*-shell Raman scattering contribution (and combine it with the elastic cross section) to properly compare with the quantities observed in Ref. [1]. A second example of resolution issues is in measurements at sufficiently low energies, where it becomes difficult to distinguish elastic scattering from inelastic scattering. The separation of the elastic and inelastic peaks becomes comparable with the width of the observed elastic peak, which is determined by detector energy resolution, so that the two peaks overlap significantly. In this situation one is observing the total of elastic and inelastic scattering, in which elastic scattering tends to be dominant, and one may focus on its proper treatment.

Let us now discuss the expected behavior of our four corrections as a function of *Z*. While there were sufficient results available for neon in the various approximations to estimate these corrections, this is not the case for all *Z*. For example, some tabulations are restricted to low-*Z* elements (e.g., form factors and inelastic scattering factors in Ref. [15]), or a switch is made to using local exchange without electron correlations for high-*Z* elements (e.g., Compton profiles in Ref. [20]), so that there are less data available for determining the corresponding corrections for high-*Z* elements.

In going to higher *Z*, one has many more electrons that are more loosely bound. At a given fairly high energy the dynamic effects associated with these electrons are small in comparison with those for inner-shell electrons. In the elastic Rayleigh case, cross sections will be well described using the (modified) form-factor approximation, and in the inelastic Compton case most cross sections will be well described using the (relativistic) impulse approximation. Therefore, one can expect dynamic effects on total cross sections to be smaller. An exception to this is large-angle, high-energy elastic scattering from high-*Z* atoms, where dynamic effects dominate the whole-atom form factor, and a dynamic treatment is necessary.

Nonlocal-exchange and electron-correlation effects are expected to be generally important for low-*Z* elements, as has been seen here for neon. This is clearly the case for the nonlocal-exchange correction, as seen from Table I, which gives the high-momentum-transfer limit of this correction for elastic scattering from various *Z*. Generally these corrections will be less important for higher *Z*, and this feature is exploited in tabulations which switch to using local exchange without electron correlations for high *Z*. But note that such effects remain of some significance at the level of precision we have been discussing.

Relativistic corrections were seen to be generally of little importance in the low-*Z* case under consideration here, though they will become increasingly important with increasing *Z*. However, since the *S*-matrix calculations are relativistic, and tabulations for high-*Z* elements tend to use the relativistic approach, one can simply begin from the relativistic standpoint, in which case relativistic effects are no longer regarded as a perturbation, but are intrinsically included in all results. In performing a perturbative analysis of nonlocal-exchange, electron-correlation, and dynamic effects without treating relativistic effects as a perturbation, for elastic Rayleigh scattering it might be preferable to use the modified form factor rather than the ordinary relativistic form factor (as it corresponds to the correct high-energy limit for forward-angle scattering [16]), and to then redefine the dynamic correction with reference to the modified form factor. For inelastic Compton scattering one would use the relativistic impulse approximation of Ribberfors [27]. We note, however, that tabulations of results using such approximations with and without nonlocal exchange and electron correlations, which would be required to estimate the perturbative corrections, are not generally available, so new calculations would be necessary.

Finally, we mention possible strategies one can imagine using in the situations where our composite approach breaks down. We identify three such situations.

(i) For inelastic scattering the composite approach breaks down for sufficiently low momentum transfers, as the impulse and inelastic-scattering-factor approximations fail in this limit, leading to large dynamic corrections. However, as seen here for neon, this is also the regime where the Compton cross section is suppressed, so this region is not so much of a concern. In these regimes it is elastic scattering that is most important, and which needs a careful treatment.

(ii) The composite approach breaks down for elastic scattering as one approaches the region of the atomic thresholds, where anomalous scattering becomes large. In this case form-factor-based corrections to the cross section are not expected to be valid. In particular, correlations will be important for the anomalous amplitudes, even influencing the positions of thresholds and resonances. However, the situation in which a subshell anomalous amplitude is large (other than the large-scattering-angle high-energy high-Z situation discussed below) is also the regime in which the electric dipole anomalous amplitudes dominate the higher-multipole anomalous contributions. Further, one expects that correlations will be most important in the low-energy electric dipole anomalous amplitude [28]. Therefore, one can imagine simply replacing the (angle-independent) nonrelativistic nonretarded anomalous electric dipole amplitude components in the S-matrix calculations with better nonrelativistic nonretarded dipole amplitudes which include nonlocal exchange and electron correlations. These could be obtained utilizing dispersion relations and the optical theorem to obtain the amplitude from photoeffect data, which includes nonlocal exchange and electron correlations. Higher-multipole amplitudes from the usual S-matrix approach would be retained (as well as relativistic and retardation components of the dipole amplitudes), as is also necessary to obtain the correct high-energy limit.

(iii) For large-angle scattering from high-Z elements at high energies, dynamic effects in elastic scattering are known to be large [16]. Therefore, in this regime a dynamic calculation of elastic scattering, as in the S-matrix approach, is necessary. One can anticipate that further effects of nonlocal exchange and electron correlation are small here, as elastic scattering is close to nuclear-Coulombic in nature [29], though nonlocal-exchange effects may still be significant at the few percent level, based on the trends seen in Table I for the bound-state normalizations. One could, therefore, imagine correcting the S-matrix results for nonlocal-exchange effects from a knowledge of the nonlocal-exchange effects in the bound-state normalizations, regarded as a perturbation to the nuclear-Coulombic results.

VII. CONCLUSIONS

We have shown how one can produce composite results for elastic and inelastic photon-atom scattering cross sections (integrated over final photon energies so as to include the whole contribution of the Compton peak), which are expected to be valid at the 1% level. With this procedure one can apply corrections to existing local independent-particle-approximation S-matrix results, to include the nonlocal-exchange and electron-correlation effects they neglect. The corrections are estimated from results using the form-factor approximation for elastic scattering, and using the impulse and inelastic-scattering-factor approximations for inelastic scattering. In doing this, one is assuming that the nonlocal-exchange and electron-correlation effects, as well as dynamic and relativistic effects, can be regarded as linearly independent perturbative corrections. There are regimes where this assumption is not valid: for low enough energies near thresholds for elastic scattering where dynamic effects in Rayleigh scattering are big, also at high energies and large angles in high-Z elements, and for low momentum transfers for inelastic scattering, where the impulse approximation fails, leading to large Compton dynamic effects as we have defined them. In such regimes our composite procedure will not be valid.

Explicit results have been given for scattering from atomic neon, in the form of corrections to the cross sections, for all scattering angles and for photon energies in the range 1–100 keV (the K-shell threshold for neon is ≈ 870 eV). Our procedure is not expected to be valid for neon for photon energies below ≈ 1 keV for elastic scattering and at any energy for inelastic scattering if the momentum transfer is low enough (where the impulse approximation fails). The nonlocal-exchange and electron-correlation corrections can be as large as $\approx 11\%$; they have recently been observed experimentally. The nonlocal-exchange correction tends to be more important for elastic scattering, and the electron-correlation correction tends to be more important for inelastic scattering. In considering going beyond these results, we have discussed how the corrections can be expected to behave as a function of the atomic number Z, and we have discussed strategies for dealing with the regimes in which the composite scheme presented here breaks down.

ACKNOWLEDGMENT

This work was supported in part by the National Science Foundation under Grant Nos. PHY-9601752 and PHY-9970293.

[1] M. Jung, R.W. Dunford, D.S. Gemmell, E.P. Kanter, B. Krässig, T.W. LeBrun, S.H. Southworth, L. Young, J.P.J. Carney, L. LaJohn, R.H. Pratt, and P.M. Bergstrom, Jr., Phys. Rev. Lett. **81**, 1596 (1998).

[2] P.P. Kane, L. Kissel, R.H. Pratt, and S.C. Roy, Phys. Rep. **140**, 75 (1986).

[3] L. Kissel, Ph.D. thesis, University of Pittsburgh, 1977 (unpublished).

[4] P.M. Bergstrom, Jr., T. Surić, K. Pisk, and R.H. Pratt, Phys. Rev. A **48**, 1134 (1993).

[5] P. M. Bergstrom, Jr., Ph.D. thesis, University of Pittsburgh, 1992 (unpublished).

[6] J.P.J. Carney, R.H. Pratt, N.L. Manakov, and A.V. Meremianin, Phys. Rev. A **61**, 042704 (2000).

[7] P.M. Bergstrom, Jr. and R.H. Pratt, Radiat. Phys. Chem. **50**, 3 (1997).

[8] W.R. Johnson and F.D. Feiock, Phys. Rev. **168**, 22 (1968).

[9] G.E. Brown, R.E. Peierls, and J.B. Woodward, Proc. R. Soc. London, Ser. A **227**, 51 (1955).

[10] I.B. Whittingham, J. Phys. A **4**, 21 (1971).

[11] I.B. Whittingham, Aust. J. Phys. **34**, 163 (1981).

[12] L. A. Wittwer, Ph.D. thesis, University of California, Davis, 1972.

[13] H.P. Hanson, F. Herman, J.D. Lea, and S. Skillman, Acta Crystallogr. **17**, 1040 (1964).

[14] J.H. Hubbell, Wm.J. Veigele, E.A. Briggs, R.T. Brown, D.T. Cromer, and R.J. Howerton, J. Phys. Chem. Ref. Data **4**, 471 (1975).

[15] J. Wang, R.O. Esquivel, V.H. Smith, Jr., and C.F. Bunge, Phys. Rev. A **51**, 3812 (1995).

[16] L. Kissel, B. Zhou, S.C. Roy, S.K. Sen Gupta, and R.H. Pratt, Acta Crystallogr., Sect. A: Found. Crystallogr. **51**, 271 (1995).

[17] J.H. Hubbell and I. Øverbø, J. Phys. Chem. Ref. Data **8**, 69 (1979).

[18] W. Franz, Z. Phys. **98**, 314 (1936).

[19] D. Schaupp, M. Schumacher, F. Smend, P. Rullhusen, and J. H. Hubbell, J. Phys. Chem. Ref. Data **12**, 467 (1983).

[20] F. Biggs, L.B. Mendelsohn, and J.B. Mann, At. Data Nucl. Data Tables **16**, 201 (1975).

[21] D.T. Cromer and J.B. Mann, Los Alamos Scientific Laboratory Report LA-3689, 1967 (unpublished).

[22] J.H. Scofield, University of California Laboratory Report No. 51326, 1973 (unpublished).

[23] J. M. Jauch and F. Rohrlich, *The Theory of Photons and Electrons* (Springer-Verlag, New York, 1976).

[24] F. Biggs, L. B. Mendelsohn, and J. B. Mann, Sandia Laboratories Report No. SAND75-51326, 1975 (unpublished). Note that the published tabulation [20] uses nonrelativistic wave functions for low *Z*.

[25] Some of the values given for form factors at high momentum transfers in Ref. [14], obtained by interpolating on the original data [D. T. Cromer (private communication to Wm. J. Veigele)], are in error by as much as $\approx 20\%$. We therefore exclude these cases ($x = 3.0, 4.0$ Å^{-1} for the neon form factor) when we interpolate on these data in order to obtain the predictions given in Table II. Even with this procedure, elastic cross sections based on the tabulation of Hubbell *et al.* [14] still have limited precision (at the $\approx 1\%$ level) for large momentum transfers, reflecting the precision of the published data in Ref. [14]. Thus the deviations of these predictions (Table II, column 5) from the ''best'' predictions (Table II, column 3) for 59.54 keV at finite angle (corresponding to large momentum transfers) do not correspond exactly to the appropriate Rayleigh corrections given in Sec. III.

[26] F. Schnaidt, Ann. Phys. (Leipzig) **21**, 89 (1934).

[27] R. Ribberfors, Phys. Rev. B **12**, 2076 (1975).

[28] In photoeffect angular distributions and cross sections, even when quadrupole effects matter, quadrupole correlations have not been found to be important, except perhaps at threshold [M.Ya. Amusia, A.S. Baltenkov, Z. Felfli, and A.Z. Msezane, Phys. Rev. A **59**, R2544 (1999); W.R. Johnson, A. Derevianko, K.T. Cheng, V.K. Dolmatov, and S.T. Manson, *ibid.* **59**, 3609 (1999)], which suggests, in consideration of the optical theorem, a similar situation for Rayleigh scattering.

[29] P.M. Bergstrom, Jr., L. Kissel, R.H. Pratt, and A. Costescu, Acta Crystallogr., Sect. A: Found. Crystallogr. **53**, 7 (1997).